MAXIMUM LIKELIHOOD ESTIMATES AND CRAMER-RAO BOUNDS FOR MAP-MATCHING BASED SELF-LOCALIZATION

Ashwin Sarma

Autonomous Systems and Technology Department
Naval Undersea Warfare Center, Newport RI 02841

ABSTRACT

We describe a method to determine (x, y, z) position of a platform located in a region where a reference bathymetry map is available. The platform can be considered an Autonomous Undersea Vehicle (AUV) equipped with a multi-beam high frequency sonar. Estimates of the heading, pitch and roll are available through the onboard inertial navigation systems (INS). An estimate of the AUV depth from the ocean surface, altitude from a Doppler Velocity Logger (DVL) as well as the sound speed at the AUV depth are also available. The position (x, y, z) is determined based on these estimates as well as time delay estimates from the beam time series. The maximum likelihood estimate (MLE) is derived and connections between previous approaches are made. Theoretically based performance predictions are compared against MLE performance in real data. The new estimator is directly linked with the relief (or information) of the map and therefore allows for a direct estimate of accuracy. This insight is critical for integrated map-matching navigation systems but has hitherto been unavailable. The new estimator of location can constrain the error growth of a purely INS-based system and lead to improved navigation.

1. INTRODUCTION

Inertial Navigation Systems onboard the AUV can provide high-quality measurements of relative quantities such as velocity and acceleration but absolute positional error is still limited by initial estimates of position and velocity at the start of the mission. Thus absolute positional error using INS measurements cannot be bounded. It is well known that combining these relative measurements with an absolute positional measurement in, say a Kalman Filter framework, can result in an absolute positional error that is both unbiased and bounded (low variance) [1, 2]. Absolute positional measurements are usually obtained through Global Positioning System (GPS) fixes or Long Baseline (LBL) methods. However, for certain long duration unmanned missions these are not an option. If a reference bathymetry map is available, map matching techniques can provide these absolute fixes.

Map-matching historically takes a set of (x, y) location estimates along with corresponding depth (z) estimates to determine the (x, y) position in the grid, denoted (x_0, y_0, z_0). Although estimates, the (x, y, z) measurements are often assumed as exact in the map-matching process. Contouring of both the reference map and the measurements is usually the first step. The set of depths for which a contour curve must be formed must first be specified. Both the measured data and the map must be contoured in the same manner. Pixels in the measured region and the map which fall on contours are considered "on" and those not on contours are "off". The process often uses binary image similarity measures, such as the Hausdorff distance, to compare the suitability of the match of the measured binary image to the binary image map. Efficient methods to compute the distances as well as search the space of possible locations have been reported [3, 4]. Measurement errors that were initially neglected are reconsidered as resulting in spurious points in the binary image. Outlier rejection methods are then applied.

The specific set of depths chosen for contouring can dramatically affect the quality of the subsequent map-matching process. As expected, fewer contours can result in rapid map-matching but poorer match quality. The quality of map-matching is limited by the (x, y, z) resolution of the measured data and the map. However neither source of error can be directly incorporated into the method. This is due to the fact that these methods operate on binary data. Working with binary data can obscure the connection between the local relief of the reference map and the measurements. Other approaches include estimates of depth gradients [5]. However such methods also do not directly consider the measurement error. Moreover, for all these methods, multiple scans are required. Relative position of the AUV for each scan must be known precisely for multiple scan methods to be accurate.

Conventional map-matching methods operate on location and depth estimates that are derived from the more fundamental quantity - time-delay (or, equivalently, path length for an approximately constant sound speed below the sonar). Assuming sufficiently accurate attitude measurements and reference map, the fundamental error in the map-matching process is the error in the path length measurements. Path length error directly determines error in localization. A direct approach in terms of this fundamental quantity is, therefore, of

0-933957-35-1

Report Documentation Page

Form Approved
OMB No. 0704-0188

1. REPORT DATE	2. REPORT TYPE	3. DATES COVERED
SEP 2007		**00-00-2007 to 00-00-2007**

4. TITLE AND SUBTITLE	5a. CONTRACT NUMBER
Maximum Likelihood Estimates And Cramer-Rao Bounds For Map-Matching Based Self-Localization	5b. GRANT NUMBER
	5c. PROGRAM ELEMENT NUMBER
6. AUTHOR(S)	5d. PROJECT NUMBER
	5e. TASK NUMBER
	5f. WORK UNIT NUMBER
7. PERFORMING ORGANIZATION NAME(S) AND ADDRESS(ES) **Naval Undersea Warfare Center,Autonomous Systems and Technology Department,Newport,RI,02841**	8. PERFORMING ORGANIZATION REPORT NUMBER
9. SPONSORING/MONITORING AGENCY NAME(S) AND ADDRESS(ES)	10. SPONSOR/MONITOR'S ACRONYM(S)
	11. SPONSOR/MONITOR'S REPORT NUMBER(S)

12. DISTRIBUTION/AVAILABILITY STATEMENT
Approved for public release; distribution unlimited

13. SUPPLEMENTARY NOTES
See also ADM002047. Presented at the MTS/IEEE Oceans 2007 Conference held in Vancouver, Canada on Sep 29-Oct 4, 2007.

14. ABSTRACT
See Report

15. SUBJECT TERMS

16. SECURITY CLASSIFICATION OF:			17. LIMITATION OF ABSTRACT	18. NUMBER OF PAGES	19a. NAME OF RESPONSIBLE PERSON
a. REPORT **unclassified**	b. ABSTRACT **unclassified**	c. THIS PAGE **unclassified**	**Same as Report (SAR)**	**10**	

interest both for insight as well as for arriving at more accurate estimators. The approach discussed here can be viewed as a *direct* maximum likelihood (ML) approach. It is unique in that it provides estimates based on both single and multiple scans. In addition, the Cramer-Rao Lower Bound (CRLB) can be determined. The CRLB directly links achievable map-matching accuracy with local relief - a result that cannot be determined via indirect methods. This information allows for proper integration with INS-based estimates. The ML estimator is shown to meet the CRLB even when applied to in-water data.

The paper is structured as follows. The geometry of the problem and the process of converting INS measurements to Universal Transverse Mercator (UTM) based measurements for each of the measurements is discussed in section 2. In section 3, the reference map, consisting of gridded (x, y, z) triplets, is interpolated using a bivariate quadratic tensor product spline [6]. The distance to the bottom along a beam can be determined via a nonlinear root-finding method. Brent's method [7], guaranteed to solve for the root, is adopted. The root is refined by recasting the problem as the solution of a quartic in t, where t is the distance to the bottom along the beam. This is possible as the root lies in a sub-rectangle of the spline interpolant. The most important advantage is that the root can be determined via an explicit algebraic equation which is amenable to differentiation.

Specifically, a maximum likelihood (ML) estimator of the true position (x_0, y_0, z_0) based on path lengths determined from each beam time series is described. It utilizes the gradient of the log-likelihood function via a conjugate gradient approach. In addition, the explicit Cramer-Rao Lower Bound can be calculated for an estimate of (x_0, y_0, z_0). These results are briefly described in Section 4. Performance on in-water data is quantified in section 5. Section 6 discusses conclusions and future work.

2. PROBLEM GEOMETRY

Figure 1b provides an aerial view of the bathymetric region in which the AUV is currently residing. The origin is defined as the lower left corner. The region need not be rectangular but is drawn that way for convenience. This model is quite useful as the Universal Transverse Mercator (UTM) coordinate system results in regions that are approximately rectangular [8]. Figure 1a shows a side view in which z_b, the depth to the local bottom, is specified. Platform location is thus completely specified by (x, y, z_b) since (x, y) relative to the reference map's origin can always be translated to absolute positional coordinates on the earth's surface.

2.1. Converting INS measurements to UTM based measurements

The body, or vehicle reference, frame is defined as follows. The positive x axis points forward along the body axis of the vehicle. The positive y axis is toward the right side and the positive z axis is down. The origin is assumed to coincide with the phase center of the transmit and receive array. Consider the unit length vector $\vec{u} = [1\,0\,0]'$. This vector is normal to the face of a forward looking sonar array, as is considered here. A beam pointing in a specific vertical and azimuthal direction can be specified by a pair of rotations of $\vec{u}$. We assume that the receive beam is first vertically steered. The vertical depression angle α is defined in radians and is negative for downward steer (i.e. clockwise rotations from the positive x axis) in the xz plane. This amounts to rotation of the vector about the y axis[1]. The rotation matrix R_α is given by:

$$R_\alpha = \begin{bmatrix} cos\alpha & 0 & sin\alpha \\ 0 & 1 & 0 \\ -sin\alpha & 0 & cos\alpha \end{bmatrix} \quad (1)$$

and $\vec{u}_\alpha = R_\alpha \vec{u}$. Next $\vec{u}_\alpha$ is rotated β radians about the z axis to the desired azimuthal direction. Clockwise rotations from the positive x axis in the xy plane are considered positive. The rotation matrix R_β is given by:

$$R_\beta = \begin{bmatrix} cos\beta & -sin\beta & 0 \\ sin\beta & cos\beta & 0 \\ 0 & 0 & 1 \end{bmatrix} \quad (2)$$

and $\vec{u}_\beta = R_\beta \vec{u}_\alpha$.

The INS provides attitude measurements - heading (γ), pitch (δ) and roll (ϵ) - describing the orientation of the body with respect to an assumed 'local' North-East-Down (NED) frame [9]. The positive x axis of NED frame lies along North in the tangent plane, positive y along the East and positive z geocentrically downward. Thus the coordinate axes of the NED frame implicitly depend on an assumed absolute position (x, y, z). Specifically, the INU self-estimate of its center of mass is used to select the local NED frame with respect to which the attitude measurements are provided.

As the NED coordinate axes are virtually unperturbed for locations near the INU self-estimate it is reasonable to assume that the specific NED frame selected by the INU (and thus the beam pointing direction vector) is *fixed* for a set of points near the INU self-estimate. Points of interest include the phase center, which may be translated from the INU center of mass, as well as all candidate positions considered in the maximum likelihood estimation process.

The beam pointing direction is completely specified with respect to the body frame through $\vec{u}_\beta$. We now wish to specify this direction with respect to the 'local' North-East-Down

[1] Some inertial navigation systems (INS) alternatively assume the positive y on the left side and positive z up. The Kearfott INS which we consider later is such an example.

(NED) frame. By Euler's theorem [9] a sequence of three rotations about coordinate axes are sufficient to rotate one coordinate frame into the other provided they share the same origin. From the previous discussion we can safely translate the origin of the NED frame from the INU center of mass to the phase center such that both the body and NED frames use the phase center as the origin.

The 'local' NED frame can be rotated to match the body frame through first rotating the NED frame in the NE plane clockwise by γ radians. This angle is the vehicle heading. The new frame is then rotated in the new xz plane upward by δ radians. This angle is the pitch. Finally the new frame is rotated in the new yz plane clockwise (as viewed from the tail end of the vehicle) by ϵ radians. This angle is the roll.

Thus any vector $\vec{u}$ defined in the NED frame can be redefined in the body frame by $R_\epsilon\, R_\delta\, R_\gamma\, \vec{u}$ where

$$R_\gamma = \begin{bmatrix} cos\gamma & sin\gamma & 0 \\ -sin\gamma & cos\gamma & 0 \\ 0 & 0 & 1 \end{bmatrix} \quad (3)$$

$$R_\delta = \begin{bmatrix} cos\delta & 0 & sin\delta \\ 0 & 1 & 0 \\ sin\delta & 0 & cos\delta \\ 0 & 0 & 1 \end{bmatrix} \quad (4)$$

$$R_\epsilon = \begin{bmatrix} 1 & 0 & 0 \\ 0 & cos\epsilon & sin\epsilon \\ 0 & -sin\epsilon & cos\epsilon \end{bmatrix} \quad (5)$$

Conversely any vector $\vec{u}$ defined in the body frame can be redefined in the NED frame by $\left[R_\epsilon\, R_\delta\, R_\gamma\right]^{-1}\, \vec{u} = R_\gamma^T\, R_\delta^T\, R_\epsilon^T\, \vec{u}$. Let us define $\vec{u}_{NED}$ as

$$\vec{u}_{NED} = R_\gamma^T\, R_\delta^T\, R_\epsilon^T\, \vec{u}_\beta \quad (6)$$

The process of determining vehicle location will utilize reference bathymetric measurements registered to a Universal Transverse Mercator (UTM) grid. The UTM grid is a projection of the spherical earth onto a cylinder. Each UTM zone is centered on a meridian and defines grid north along it [8]. The origin of each zone is at the intersection of the equator and the center meridian. Note that for the UTM coordinate system the northing axis is the y axis and the easting the x axis.

Thus points along the central meridian will be represented as points along the y axis in the grid. Note that for points in the zone not along the central meridian the north and east directions corresponding to the local NED coordinate frame are rotated with respect to grid north and east. For points west of the central meridian true north is east of grid north and vice versa. The rotation angle η can be determined by determining the UTM zone locations $(x_1, y_1), (x_2, y_2)$ for two points with the same longitude but slightly different latitudes and defining η as

$$\eta = \tan^{-1}\left(\frac{x_2 - x_1}{y_2 - y_1}\right) \quad (7)$$

Selecting (x_1, y_1) at the INU estimate of the phase center should lead to an accurate estimate of η.

The vector $\vec{u}_{NED}$, redefined in the rotated UTM coordinate system, is denoted $\vec{u}_{UTM}$ and is given by

$$\vec{u}_{UTM} = R_\eta\, \vec{u}_{NED} \quad (8)$$

where

$$R_\eta = \begin{bmatrix} cos\eta & -sin\eta & 0 \\ sin\eta & cos\eta & 0 \\ 0 & 0 & 1 \end{bmatrix} \quad (9)$$

Although $\vec{u}_{UTM}$ is defined with respect to the UTM system we note that the first element of $\vec{u}_{UTM}$ corresponds to the component of the beam pointing ray along grid north, the second element corresponds to the component along grid east and the third element corresponds to the component along the downward z axis. A final rotation of the coordinate system is required to specify that the easting component is the x component, the northing component is the y and the upward normal is the z component. The vector $\vec{v} = [v_x\, v_y\, v_z]'$ reflecting this rotation is given by

$$\vec{v} = R\, \vec{u}_{UTM} \quad (10)$$

where

$$R = \begin{bmatrix} 0 & 1 & 0 \\ 1 & 0 & 0 \\ 0 & 0 & -1 \end{bmatrix} \quad (11)$$

Thus the beam direction is now completely described by the vector $\vec{v}$.

3. ESTIMATING THE DISTANCE TO THE BOTTOM ALONG A BEAM

The intersection of the ray along $\vec{v}$ with the bottom must occur at $(x_0 + tv_x, y_0 + tv_y, z_0 + tv_z)$ for some t. An estimate of the path length t, denoted $\hat{t}$, can be obtained by finding the smallest positive root of the function

$$f(t) = Z(t) - (z_0 + tv_z) \quad (12)$$

where $Z(t) = Z(x, y)$ is the depth Z of the ocean floor at $(x, y) = (x_0 + tv_x, y_0 + tv_y)$. The function $Z(x, y)$ is assumed to be a bivariate quadratic spline interpolation[2] of the N database measurements $(x_i, y_i, z_i),\ i = 1, ..., N$. Tensor product splines are well-suited for interpolation of gridded data as is available in most bathymetric databases. The bivariate quadratic spline interpolation is an instance of a tensor product spline.

A rapid root finding routine with guaranteed convergence such as Brent's method [7] can be applied to obtain $\hat{t}$. This routine is known as *fzero* in Matlab [10]. This is performed for each of the beams.

[2]The MATLAB Spline toolbox routine *spapi.m* is used

3.1. Refining the estimate: Solving for the exact roots of the quartic

The sea floor depth in each sub-rectangle of the grid is approximated by a bivariate polynomial in x and y of degree n in x and m in y [6]. In our case the degree in both dimensions is equal to 2, or we have a quadratic in x for y fixed and vice versa.

It is clear that $(x(\hat{t}), y(\hat{t}))$ falls within a specific sub-rectangle. Denote the bivariate quadratic polynomial describing the depth for points in this sub-rectangle as

$$p(x,y) = \sum_{i=0}^{2}\sum_{j=0}^{2} a_{ij}\,(x-x_a)^{2-i}(y-y_a)^{2-j}. \qquad (13)$$

where x_a and y_a specify the location of the lower left corner of the sub-rectangle.

If we consider only points $(x,y) = (x(t), y(t)) = (x_0 + tv_x, y_0 + tv_y)$ the corresponding depth $p(t)$ is a quartic in t. Thus the exact root of interest must be one of the four roots of the related quartic equation

$$q(t) = p(t) - (z_0 + tv_z) = at^4 + bt^3 + ct^2 + dt + e = 0. \quad (14)$$

After some algebra the coefficients can be obtained as

$$\begin{aligned}
a &= a_{00}\,{v_x}^2{v_y}^2 \\
b &= 2a_{00}\,v_x{v_y}^2(x_0-x_a) + 2a_{00}\,{v_x}^2v_y(y_0-y_a) + \\
&\quad a_{01}\,{v_x}^2v_y + a_{10}\,v_x{v_y}^2 \\
c &= a_{00}\,{v_y}^2(x_0-x_a)^2 + a_{00}\,{v_x}^2(y_0-y_a)^2 + \\
&\quad 4a_{00}\,v_xv_y(x_0-x_a)(y_0-y_a) + 2a_{01}\,v_xv_y(x_0-x_a) + \\
&\quad a_{01}\,{v_x}^2(y_0-y_a) + 2a_{10}\,v_xv_y(y_0-y_a) + \\
&\quad a_{10}\,{v_y}^2(x_0-x_a) + a_{11}\,v_xv_y + a_{02}\,{v_x}^2 + a_{20}\,{v_y}^2 \\
d &= 2a_{00}\,v_y(x_0-x_a)^2(y_0-y_a) + \\
&\quad 2a_{00}\,v_x(x_0-x_a)(y_0-y_a)^2 + a_{01}\,v_y(x_0-x_a)^2 + \\
&\quad 2a_{01}\,v_x(x_0-x_a)(y_0-y_a) + a_{10}\,v_x(y_0-y_a)^2 + \\
&\quad 2a_{10}\,v_y(x_0-x_a)(y_0-y_a) + a_{11}\,v_x(y_0-y_a) + \\
&\quad a_{11}v_y(x_0-x_a) + 2a_{02}\,v_x(x_0-x_a) + \\
&\quad 2a_{20}\,v_y(y_0-y_a) + a_{12}\,v_x + a_{21}\,v_y - v_z \\
e &= a_{00}\,(x_0-x_a)^2(y_0-y_a)^2 + a_{01}\,(x_0-x_a)^2(y_0-y_a) + \\
&\quad a_{10}\,(x_0-x_a)(y_0-y_a)^2 + a_{11}\,(x_0-x_a)(y_0-y_a) + \\
&\quad a_{02}\,(x_0-x_a)^2 + a_{20}\,(y_0-y_a)^2 + a_{12}\,(x_0-x_a) + \\
&\quad a_{21}\,(y_0-y_a) + a_{22} - z_0 \qquad (15)
\end{aligned}$$

The quartic is the highest degree general polynomial whose roots can be obtained via analytical expressions. The choice of a quadratic spline fit directly led to this result. In addition, we observe that these expressions are *explicit algebraic functions* [11], i.e. functions of a finite number of algebraic and root extraction operations.

It can be seen that at least two of the four roots are real valued. Our estimate $\hat{t}$ will correspond to one of these roots. In the calculation of the root, intermediate quantities are sometimes complex valued. We choose to view all functions involved in determining the root as extended in a complex sense. As algebraic operations as well as the multi-valued square and cube rooting functions are analytic [12] general complex differentiation is possible. A function which is a composition of other analytic functions is itself analytic. This allows application of the chain rule as well as evaluation of specific partials at points along the real line when required. However imaginary components must ultimately vanish as the partial derivatives must be real valued.

The expressions for the roots, associated partial derivatives and details for their evaluation are lengthy. They shall be included in a more detailed correspondence. The next section will reveal how these partial derivatives are used to realize the MLE and the CRLB.

4. MAXIMUM LIKELIHOOD ESTIMATOR OF (X_0, Y_0, Z_0)

The time-delay measurements from each of the beams of our forward-looking (or bottom-looking or side-scan) sonar as well as the Doppler Velocity Logger altitude estimate form the raw data for the MLE. Time delays are converted to one-way distances to the bottom through the local sound speed - assumed fixed and known. This is certainly a reasonable assumption as most map-matching applications operate over short ranges. This is since signal to noise ratios generally degrade rapidly as the distance to the bottom increases. The total number of measurements is denoted B. Note that given bathymetric information, the distance along a beam is completely defined by the position (x,y,z) and the beam pointing direction $\vec{v}$. We assume that $\vec{v}$ is known for all B measurements and that the distance measurements are unbiased.

Denote the B distance measurements as $d_1, ..., d_B$. Assuming all measurements are statistically independent and Gaussian but not necessarily identically distributed leads to the log-likelihood function L

$$L = \sum_{i=1}^{B} -\frac{(d_i - t_i)^2}{2{\sigma_i}^2} \qquad (16)$$

in which terms independent of (x,y,z) have been discarded.

Note that the variance on each measurement is dependent on the sonar orientation. Specifically for a bottom looking configuration the variance is expected to be rather small while for a forward looking configuration the variance is expected to be rather large. The actual distance along the beam to the bottom also affects the variance. Longer distances are expected to lead to larger variances. Representative numbers for these measurements must be provided in order for the MLE and the CRLB to be useful.

The partial derivatives of L w.r.t. x, y and z are:

$$\frac{\partial L}{\partial x} = \sum_{i=1}^{B} \frac{(d_i - t_i)}{{\sigma_i}^2} \frac{\partial t_i}{\partial x} \quad (17)$$

$$\frac{\partial L}{\partial y} = \sum_{i=1}^{B} \frac{(d_i - t_i)}{{\sigma_i}^2} \frac{\partial t_i}{\partial y} \quad (18)$$

$$\frac{\partial L}{\partial z} = \sum_{i=1}^{B} \frac{(d_i - t_i)}{{\sigma_i}^2} \frac{\partial t_i}{\partial z} \quad (19)$$

The gradient is then $grad\, L = \frac{\partial L}{\partial x}\vec{i} + \frac{\partial L}{\partial y}\vec{j} + \frac{\partial L}{\partial z}\vec{k}$. The gradient is used to implement a conjugate gradient procedure to find the maximum of L. The Polak-Ribiere update is used [13]. Iterations cease when L changes by less than 0.01%.

Second order partials are not required to calculated the CRLB but are useful to check whether a solution ($grad\, L = 0$) is at least a local maximum. Specifically, if the 3 x 3 Hessian matrix of L is negative definite (i.e. all eigenvalues are negative) we are at a local maximum.

4.1. Fisher Information Matrix and CRLB at (x_0, y_0, z_0)

Every unbiased estimator of the true position (x, y, z) that operates on these B measurements must possess an error covariance matrix C such that $C - J^{-1}$ is non-negative definite provided J^{-1} exists. Here J is the 3 x 3 Fisher Information Matrix with elements:

$$J_{11} = \sum_{i=1}^{B} \frac{1}{{\sigma_i}^2} \Big(\frac{\partial t_i}{\partial x}\Big)^2 \quad (20)$$

$$J_{22} = \sum_{i=1}^{B} \frac{1}{{\sigma_i}^2} \Big(\frac{\partial t_i}{\partial y}\Big)^2 \quad (21)$$

$$J_{33} = \sum_{i=1}^{B} \frac{1}{{\sigma_i}^2} \Big(\frac{\partial t_i}{\partial z}\Big)^2 \quad (22)$$

$$J_{12} = \sum_{i=1}^{B} \frac{1}{{\sigma_i}^2} \frac{\partial t_i}{\partial x} \frac{\partial t_i}{\partial y} = J_{21} \quad (23)$$

$$J_{13} = \sum_{i=1}^{B} \frac{1}{{\sigma_i}^2} \frac{\partial t_i}{\partial x} \frac{\partial t_i}{\partial z} = J_{31} \quad (24)$$

$$J_{23} = \sum_{i=1}^{B} \frac{1}{{\sigma_i}^2} \frac{\partial t_i}{\partial y} \frac{\partial t_i}{\partial z} = J_{32} \quad (25)$$

$$(26)$$

The CRLB can reveal how well we can estimate position in a hypothesized location, eg. at the current best estimate. We will see that the implementation of the MLE via the conjugate gradient appears to meet the CRLB. In this case J^{-1} also serves as the measurement noise covariance for incorporation into a Kalman Filter.

5. PERFORMANCE

Data were collected in the Narragansett Bay, RI using a 48 beam Reson 7012 forward-looking sonar mounted on a AUV equipped with the Kearfott INS and a Doppler Velocity Logger (DVL). The total number of measurements, denoted B, includes the 48 sonar beams as well as the DVL altitude measurement. A rough estimate of the sonar depth is also available. A bathymetric database with 5 meter resolution in both x and y was used to form the reference map. Sonar beams were steered 15° downward and spanned an azimuthal sector of 120° with 2.5° spacing. The DVL altitude error has a standard deviation of 0.1 m [14]. The coefficient of variation (ratio of standard deviation to mean) of the estimated time-delays is 0.05. Thus the Reson path-length error has a standard deviation of $0.05t$. Assuming a flat-bottom allows us to approximate the standard deviation of the error via the altitude estimate.

The AUV travels in a north-south manner over a region with a relatively deep bottom. This region, known as "the hole", is shown in Figure 2. Gould Island is on the left side of the figure. The point notes the location at which map-matching was performed. Figure 3 plots the 48 beam time series along with the locations of the time-delay estimates (white *) in terms of sample number. These estimates are chosen as the peak magnitude of each time series. The white dashed curve corresponds to the expected sample locations based on the INS estimate. The white solid curve corresponds to the expected sample locations based on the MLE map-matching estimate. Note that the time-delay estimates become poorer for beams numbered greater than 35. This is due to a lower signal-to-noise ratio in these beams. The log-likelihood function L uses an L_1 norm ($|d_i - t_i|$) instead of the L_2 norm ($(d_i - t_i)^2$). The L_1 norm is preferred as it is less sensitive to outliers and sacrifices little performance in outlier-free situations. It is closely linked with the double-exponential distribution - a reasonable model for heavy-tailed error.

The assumed location of the AUV based on the integrated INS/DVL estimate is denoted (x_0, y_0, z_0). Here (x_0, y_0) correspond to the output of the integrated kalman filter and z_0 is the altitude estimate corrected for tidal variations to match the database datum. The location (x_0, y_0) is shown in Figure 4 along with the Circular Error Probability ellipse. It is reasonable to assume that the true location lies somewhere in the CEP_{90} ellipse.

Conjugate Gradient methods require an initial guess. In an operational setting a reasonable choice would be (x_0, y_0, z_0). It is clear from the CRLB that the resolution in the z dimension exceeds that in x and y. This is as expected as the DVL estimate provides an accurate estimate of altitude. When the maximization routine does not search over z the MLE is less than 5 meters from (x_0, y_0, z_0). Based on J^{-1} the 2σ ellipse (coverage of 87%) contains the MLE. When instead a

set of possible altitudes within the range of possible error are pre-selected and the conjugate gradient routine finds the best (x, y) for a specific z and the (x, y, z) solution corresponding to the maximum likelihood is selected, the estimate (denoted as *) is less than 3 meters from (x_0, y_0, z_0). In this case the 1σ ellipse (coverage of 39%) contains the MLE. Results from other scans, including those taken in low-relief areas, again suggested that the estimator is *efficient* - i.e. meets the CRLB [15].

With an fully operational DVL it is reasonable to assume that an accurate estimate of z is available. However, for long straight runs the x and y INS estimates will steadily degrade. As the conjugate gradient methods are not guaranteed to find the global maximum it is possible that an initial guess far from the true location can result in a poor estimate. In order to determine how the estimator performs when the initial guess for x and y is much poorer than (x_0, y_0) the experiment was repeated with an intial choice of $(x_0 + 100, y_0 - 100, z_0)$. This choice is approximately 141 meters away from the true location of the AUV. The result from the ML map-matching routine is shown in Figure 4 (black square). Note that the result still lies within the 2σ ellipse based on the CRLB suggesting that the quality of the initial guess is not overly critical to the successful operation of the estimator.

6. CONCLUSIONS

Due to the strong connection with the fundamental error in the map-matching process and the relation to the CRLB the estimator should be practically equivalent to the minimum variance unbiased estimator. A cursory examination of the performance of image-based map-matching methods corroborates this. An important benefit of the explicit CRLB is the ability to evaluate the bound at the INS estimate. If the maximum performance improvement from map-matching is poor, map-matching need not be performed to save on processing. As the trajectory is approximately known in advance, locations where map-matching will be of benefit can be selected apriori. The ML estimator and the CRLB are defined for both the single-scan and multiple-scan case. Relative position of the AUV for each scan must be known precisely for multiple scan methods to be accurate. Thus the single scan case appears better suited for Kalman Filter integration. These issues will be discussed in a detailed correspondence.

7. ACKNOWLEDGEMENT

Thanks to Robert Carpenter for contributions that greatly improved the manuscript.

8. REFERENCES

[1] Marvin B. May, "Inertial Navigation and GPS," *GPS World*, pp. 56–66, September 1993.

[2] Mohinder P. Grewal, L.R. Weill, and A.P. Andrews, *Global Positioning Systems, Inertial Navigation and Integration*, Wiley-Interscience, 2000.

[3] Clark F. Olson, "Probabilistic self-localization for mobile robots," *IEEE Transactions on Robotics and Automation*, vol. 16, pp. 55–66, 2000.

[4] Robert N. Carpenter and Michael R. Medeiros, "Concurrent mapping and localization and map matching on autonomous underwater vehicles," in *Proceedings of the MTS/IEEE Oceans Conference, Honolulu, HI*, 2001.

[5] L. Lucido, J. Opderbecke, V. Rigaud, R. Derice, and Z. Zhang, "A terrain referenced underwater positioning using sonar bathymetric profiles and multiscale analysis," in *Proceedings of the MTS/IEEE Oceans Conference, Fort Lauderdale, FL*, 1996.

[6] Paul Dierckx, *Curve and Surface Fitting with Splines*, Oxford Science Publications, New York, 1993.

[7] R.P. Brent, *Algorithms for minimization without derivatives*, Prentice Hall, Englewood Cliffs, New Jersey, 1973.

[8] Michael Ferguson, *GPS Land Navigation: A Complete Guidebook for Backcountry Users of the NAVSTAR Satellite System*, Glassford Publishing, Boise, Idaho, 1997.

[9] Jack B. Kuipers, *Quaternions and Rotation Sequences*, Princeton University Press, NJ, 1999.

[10] David Kahaner, Cleve Moler, and Stephen Nash, *Numerical Methods and Software*, Prentice Hall, New Jersey, 1989.

[11] Godfrey Harold Hardy, *A Course of Pure Mathematics*, Cambridge, UK, tenth edition, 1958.

[12] E.C. Titchmarsh, *The Theory of Functions*, Oxford University Press, second edition, 1939.

[13] W.H. Press, S.A. Teukolsky, W.T. Vettering, and B.P. Flannery, *Numerical Recipies in C: The Art of Scientific Computing*, Cambridge University Press, second edition, 1994.

[14] W. Alameda, "Seadevil: A totally integrated inertial navigation solution," in *Underwater Intervention Symposium, New Orleans LA*, 2002.

[15] L. L. Scharf, *Statistical Signal Processing: Detection, Estimation and Time Series Analysis*, Addison-Wesley: Reading Massachusetts, 1991.

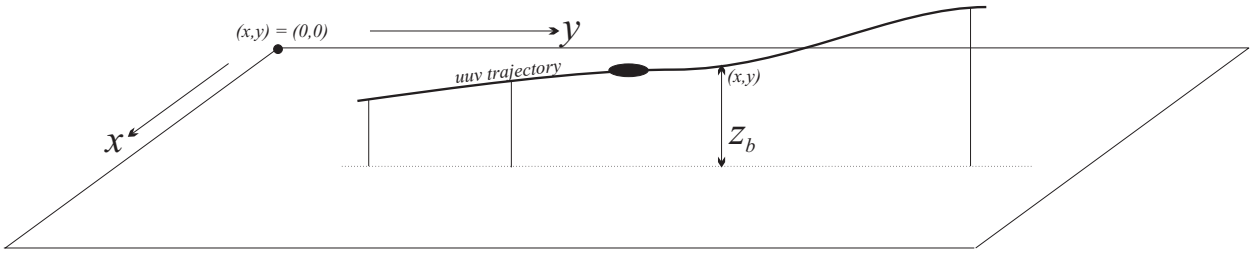

(a)

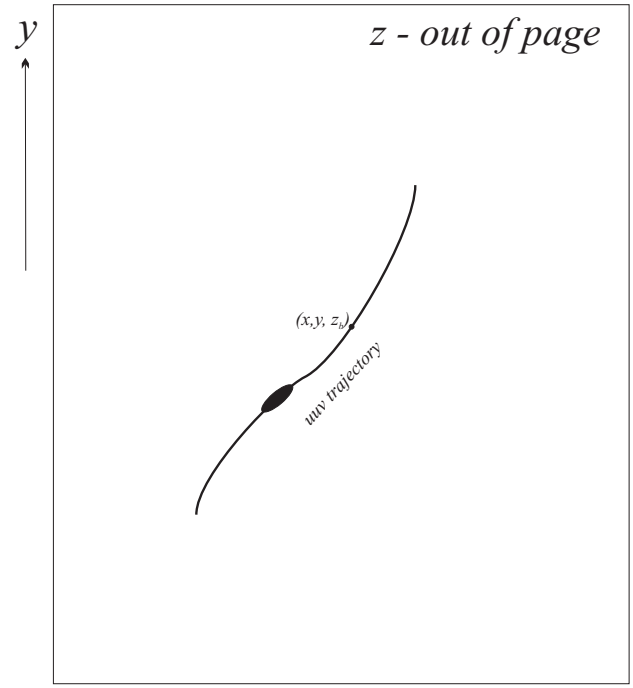

(b)

Fig. 1. Geometry

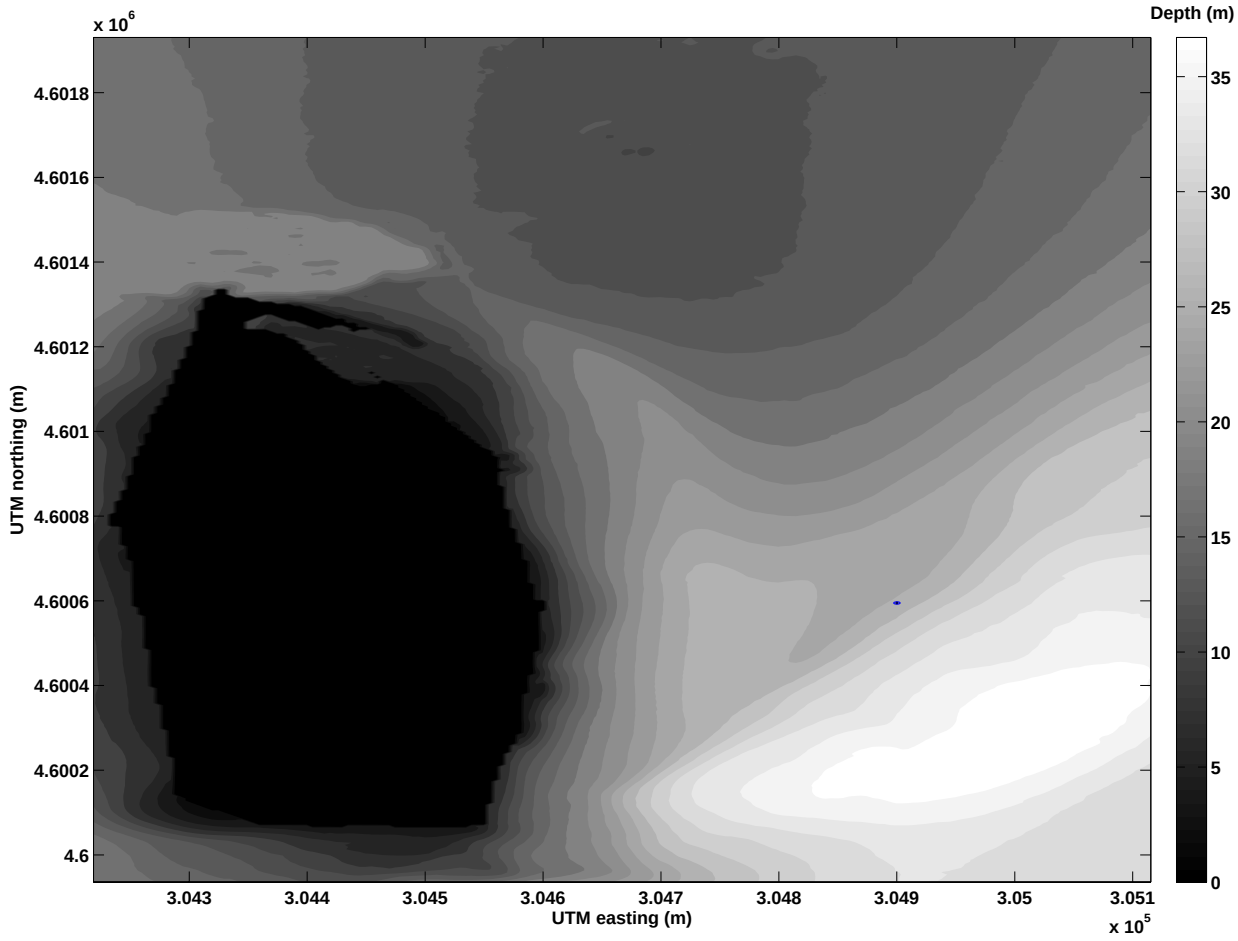

Fig. 2. Narragansett Bay, RI - test site

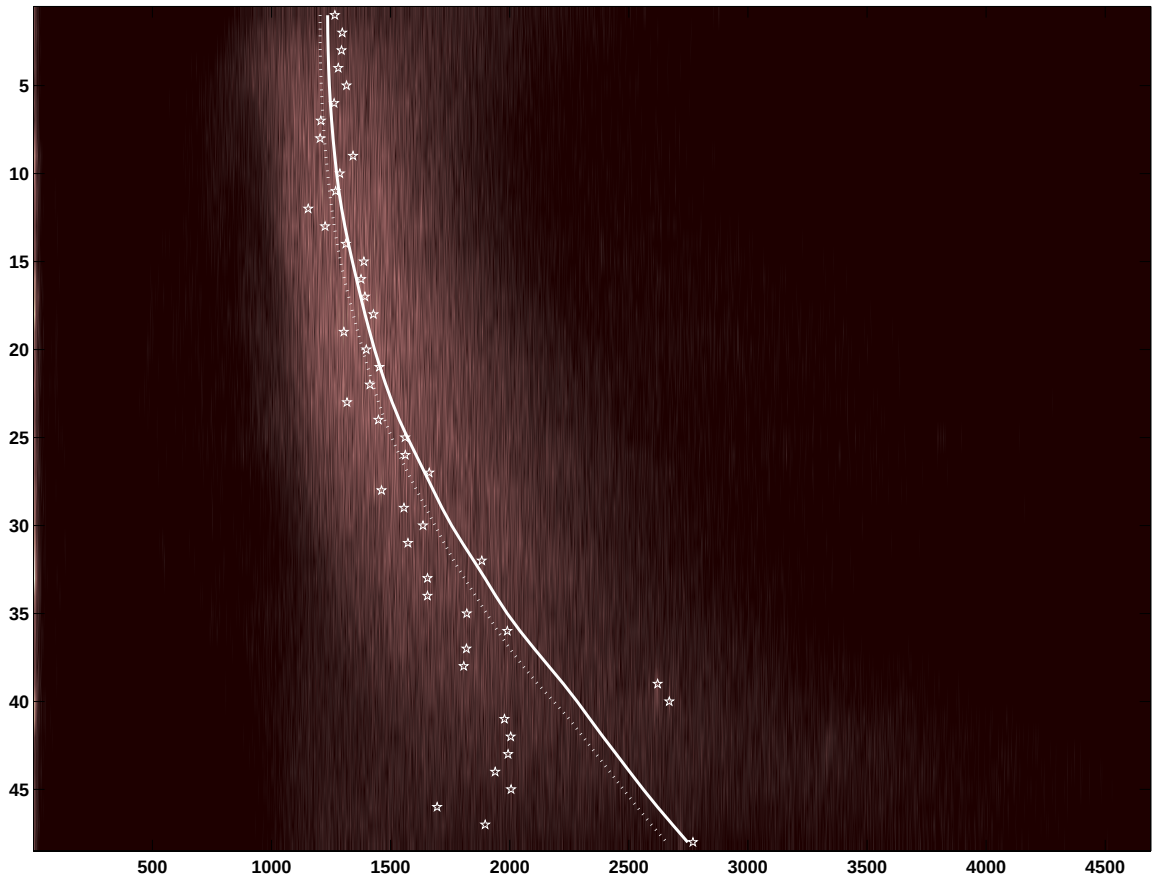

Fig. 3. time series for 48 beams and time-delay estimates

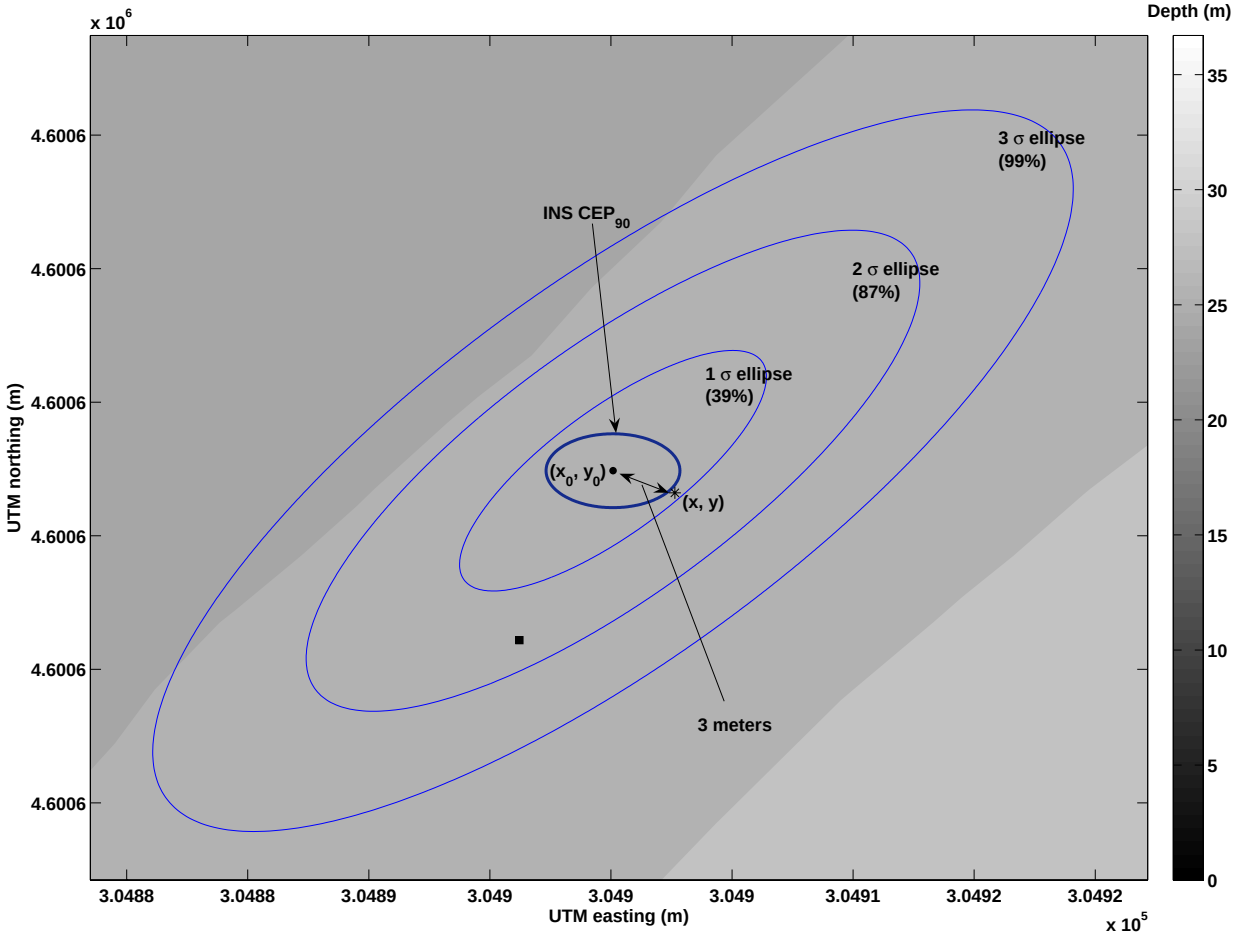

Fig. 4. map-matching results and comparison to CRLB